Electron Paramagnetic Resonance Analysis of Different *Azotobacter vinelandii* Nitrogenase MoFe-Protein Conformations Generated during Enzyme Turnover: Evidence for $S = {}^3/_2$ Spin States from Reduced MoFe-Protein Intermediates†

Karl Fisher,‡ William E. Newton,*,‡ and David J. Lowe*,§

Department of Biochemistry, The Virginia Polytechnic Institute and State University, Blacksburg, Virginia 24061, and Nitrogen Fixation Laboratory, John Innes Centre, Norwich NR4 7UH, U.K.

Received June 2, 2000; Revised Manuscript Received January 9, 2001

ABSTRACT: Rapid-freezing experiments elicited two transient EPR signals, designated 1b and 1c, during *Azotobacter vinelandii* nitrogenase turnover at 23 °C and pH 7.4. The first of the signals to form, signal 1b, exhibited *g* values of 4.21 and 3.76. Its formation was at the expense of the starting EPR signal (signal 1a with *g* values of 4.32, 3.66, and 2.01). The second signal to arise, signal 1c, with a characteristic *g* value of 4.69, formed very slowly and was always of low intensity. Both signals occurred independently of the substrate being reduced. Increased electron flux through the MoFe protein caused these signals to form more rapidly. Moreover, after a MoFe-protein solution had been pretreated (using conditions of extremely low electron flux) to set up an equimolar mixture of its resting state and one-electron reduced state, these signals appeared even more rapidly when this mixture was exposed to an excess of the Fe protein. We have simulated the kinetics of formation of these EPR features using the published kinetic model for nitrogenase catalysis [Lowe, D. J., and Thorneley, R. N. F. (1984) *Biochem. J. 224*, 887−909] and propose that they arise from reduced states of the MoFe protein and reflect different conformations of the FeMo cofactor with different protonation states.

The metalloenzyme commonly known as nitrogenase catalyzes the biological reduction of dinitrogen (N_2) to ammonia (NH_3). The Mo-based nitrogenase system contains two easily separable component proteins, the MoFe protein[1] and the Fe protein. The larger (230 kDa) $\alpha_2\beta_2$ MoFe protein contains two 7Fe-Mo-9S-homocitrate centers, called the FeMo cofactors, and two 8Fe7S centers, called the P clusters. The crystal structure reveals that only α-442^{His} and α-275^{Cys} ligate the FeMo cofactor, whereas each P cluster lies at an $\alpha\beta$-subunit interface and is ligated by residues from both subunits (*1*, *2*). The nitrogenase substrate-binding and -reduction site(s) is generally agreed to be on the FeMo-cofactor center of the MoFe protein (*3*−*5*). The smaller (63 kDa) Fe protein is a γ_2-homodimer, which contains a single Fe_4S_4 cluster that bridges the two subunits (*6*). Under in vitro assay conditions, the reduced Fe protein, which is the only known reductant for the MoFe protein, transfers electrons at the expense of MgATP hydrolysis with usually two molecules of MgATP hydrolyzed for every electron that is transferred (*7*).

Both nitrogenase proteins, together with an anaerobic environment, a suitable reducing source, and MgATP, are essential for substrate reduction. The mode(s) of interaction of substrates with the metal centers remains a mystery, although some progress in understanding the binding of the inhibitor, CO, has been made (*8*−*11*). However, a detailed scheme that accounts for nitrogenase kinetics has been described (*12*). This scheme comprises the association of the two nitrogenase proteins, electron transfer from the Fe protein to the MoFe protein coupled with MgATP hydrolysis, and protein−protein dissociation. A number of electron-transfer cycles must be completed to reduce the substrate by multiple electrons because no substrate is reduced to product in a single electron-transfer event. Accumulation of increasing numbers of electrons by the MoFe protein results in different redox levels being assumed by the MoFe protein. These redox levels are termed E_n, where *n* is the number of electrons that have been accepted relative to the resting state of the MoFe protein (E_0) as prepared in the presence of dithionite. Under conditions of very low electron flux, i.e., with a very low Fe protein:MoFe protein molar ratio, the single-electron-reduced MoFe protein species (E_1) accumulates until the concentrations of E_0 and E_1 are essentially equal, whereas any two-electron-reduced species (at the E_2

† Support from the National Institutes of Health (Grant DK 37255 to W.E.N.) and the United Kingdom's BBSRC (to D.J.L.) is gratefully acknowledged.

* To whom correspondence should be addressed. W.E.N.: telephone, (540) 231-8431; fax, (540) 231-9070; e-mail, wenewton@vt.edu. D.J.L.: telephone, +(44) 1603 450742; fax, +(44) 1603 450018; e-mail, david.lowe@bbsrc.ac.uk.

‡ The Virginia Polytechnic Institute and State University.

§ John Innes Centre.

[1] Abbreviations: Fe protein, iron protein of nitrogenase; L127Δ, iron protein of nitrogenase with residue Leu 127 deleted; MoFe protein, molybdenum−iron protein of nitrogenase; E_n, general designation for the different redox states of the MoFe protein, where *n* is the number of electrons that have been transferred to it relative to the protein as prepared in the presence of dithionite, which is called E_0; EPR, electron paramagnetic resonance; EXAFS, extended X-ray absorption fine structure; PTFE, polytetrafluoroethylene; MgATP, magnesium salt of adenosine triphosphate; HEPES, *N*-(2-hydroxyethyl)piperazine-*N*′-2-ethanesulfonic acid; SDS−PAGE, sodium dodecyl sulfate−polyacrylamide gel electrophoresis; EDTA, ethylenediaminetetraacetic acid.

10.1021/bi0012686 CCC: $20.00
Published on Web 02/24/2001

redox level) that is formed reverts to the resting enzyme by evolving H_2 (*13*). At higher electron flux, H_2 is evolved from the three- and four-electron-reduced MoFe-protein species, redox levels E_3 and E_4, respectively. It is believed that the reduced MoFe protein must dissociate from the Fe protein before it can bind substrates and release products (*14*). Although these various reduced MoFe-protein species have been invoked during turnover, most of these transients have been characterized only by the kinetics of product formation.

Spectroscopy has played an important role in elucidating the structure and properties of the nitrogenase metal clusters. The EPR spectrum of the resting (E_0 level) MoFe protein is rhombic in shape with *g* values of approximately 4.3, 3.7, and 2.0. This signal originates from the FeMo cofactors and is interpreted as arising from an $S = \pm^1/_2$ ground-state Kramers doublet of a spin $S = {}^3/_2$ system (*15*−*17*). EPR and Mössbauer studies have shown that, when dithionite is used as the reducing source in vitro, the Fe protein transfers one electron at a time to the MoFe protein, and ultimately to the substrate, during catalysis (*18*−*20*). During this event, the EPR spectra of both the Fe protein and the MoFe protein become bleached as the proteins become oxidized and reduced, respectively. Multiple variations of the $S = {}^3/_2$ signal have been observed for the MoFe protein from *Klebsiella pneumoniae* (*21*). A signal, designated as Ia with *g* values of 4.32, 3.63, and 2.01, occurs at neutral pH in the resting MoFe protein. Another signal, signal Ib, has lower rhombicity, with *g* values of 4.27, 3.73, and 2.02, and is observed at higher pH. A third signal, signal Ic, with even higher rhombicity and *g* values of 4.67, 3.37 and 2.0, is only observed during turnover. In addition, EPR signals that are associated with the MoFe protein in the presence of either CO (*11*, *22*) or C_2H_2 and C_2H_4 (*21*) have been described. Furthermore, several altered MoFe proteins, containing specific substitutions in the FeMo-cofactor environment, also display additional EPR features in their resting states (*23*, *24*). These last signals have been suggested to represent either trapped turnover intermediates or FeMo cofactors bound in different conformations.

The solution and continuing refinement of the MoFe-protein crystal structure has produced a reasonable understanding of the distribution and likely function of the metal clusters in the resting state (*2*, *25*−*28*). Knowledge of the crystal structure of the resting state of this protein is important for designing experiments to probe the nitrogenase mechanism, but it does not describe the form(s) of the enzyme present during catalysis. Many metalloproteins undergo substantial structural changes either during redox or on ligand binding. The crystal structure of the MoFe protein in a tight complex with the Fe protein has been determined, using either MgADP·AlF_4 or the L127Δ Fe protein to simulate the ATP-bound, but nonhydrolyzable, form of the Fe protein (*29*−*32*). However, these structures indicate that only relatively minor structural changes occur within the environment of the MoFe-protein metal clusters on complex formation. Unfortunately, due to procedures inherent in obtaining crystals, the redox state(s) of the clusters within the crystallized proteins is unknown. Extended X-ray absorption fine structure (EXAFS) data also show that the overall interatomic distances within the FeMo cofactor change very little on reduction to the one-electron-reduced state (*33*). Even so, the fact that the FeMo cofactor is only constrained by ligation to two amino acid residues with an undercoordinated midsection suggests flexibility and ample opportunity for structural change during catalysis.

Because numerous redox states, most of which would be inaccessible to crystallography, are likely produced during turnover, many questions about the structure cannot be addressed by X-ray crystallography alone. In this investigation, we used rapid-mixing/rapid-freezing techniques and EPR spectroscopy to explore (i) any changes in the electronic structure of the MoFe protein that occur during the pre-steady-state phases of nitrogenase turnover and (ii) indications of changes in either the conformation or protonation of the FeMo cofactor itself.

EXPERIMENTAL PROCEDURES

Cell Growth and Purification of Nitrogenase Proteins. Cells of *Azotobacter vinelandii* strain DJ527 were grown in a 24 L fermenter at 30 °C in a modified liquid Burk medium (*34*). The nitrogenase Fe protein and MoFe protein were purified from these cells as described previously (*35*) and concentrated using an Amicon pressure dialysis apparatus. All protein solutions contained 25 mM HEPES (pH 7.5), 100 mM NaCl, 10 mM $MgCl_2$, and 2 mM sodium dithionite. SDS−PAGE (12% polyacrylamide containing 1.35% cross-linker with 4% stacking gel) gels stained with Coomassie Blue confirmed that the purified proteins were homogeneous (*36*). Protein concentrations were determined by the method of Lowry et al. (*37*). Using inductively coupled plasma atomic emission spectroscopy with a Perkin-Elmer Plasma 400 spectrometer (Norwalk, CT), metal analysis showed that the MoFe protein contained 1.9 ± 0.1 mol of Mo/mol with an Fe:Mo atomic ratio of 15:1. Purified Fe and MoFe proteins had maximum specific activities of 2000 and 2600 nmol of H_2 min^{-1} (mg of protein)$^{-1}$, respectively, at 30 °C.

Nitrogenase Activity Assays. Assays were carried out under an argon atmosphere in 9.25 mL reaction vials fitted with butyl rubber septa held by aluminum crimp-seal caps. Assays contained 1 mg of total protein, 10 μmol of creatine phosphate, 25 μmol of HEPES buffer (pH 7.4), 20 μmol of sodium dithionite, 2.5 μmol of ATP, 5 μmol of $MgCl_2$, and 25 units of creatine phosphokinase in a final volume of 1 mL. Assays were conducted either at 23 °C with the component protein ratios used in the rapid-freeze experiments or at 30 °C with an optimal amount of the purified complementary protein. The specific activities obtained at 23 °C were required to simulate, using the Lowe−Thorneley scheme (*12*), the proportions of the different redox states of the MoFe protein present during catalysis. Reactions were initiated by the addition of Fe protein and were terminated by injection of 0.25 mL of 0.5 M EDTA-Na_2 (pH 7.5). H_2 production was quantified by gas chromatography using a molecular sieve 5A column (Supelco, Bellefonte, PA) and a thermal conductivity detector (Shimadzu, Tokyo, Japan). Calibration was performed with a standard 1% H_2 in N_2 (Scott Specialty Gases, Plumsteadville, PA).

Rapid-Freeze Sample Preparation for EPR. The apparatus used in this study is essentially that described by Gutteridge et al. (*38*) with full anaerobic precautions as described by Bray et al. (*39*). An electronically controlled stepping motor expels a preset volume of solution from each reaction syringe at a predetermined rate. The solutions travel through a mixing

chamber and down a length of thick-walled nylon capillary tubing of variable length ending in a needle jet. The length of this capillary tubing determines the time the reaction is allowed to proceed before quenching takes place. All reaction tubes are cleaned and then flushed with N_2 before each shot. The needle jet is situated immediately above a quartz EPR tube (3.0 mm inside diameter) that is attached to a small glass funnel via a piece of removable rubber tubing. The EPR tube and funnel are seated in an isopentane bath cooled to −140 °C with liquid nitrogen. The isopentane contained within the funnel is flushed with N_2 gas immediately before sample preparation to remove any dissolved oxygen. After freezing, the protein reaction mix is packed tightly into the bottom of the EPR tube with a PTFE-tipped packing rod. The EPR tube is then detached from the funnel and stored in liquid N_2 ready for EPR analysis. The experimental series was performed three times with duplicate samples prepared for each time point. EPR spectra were recorded on the day of preparation. Unless otherwise stated, one of the reaction syringes contained MoFe protein and Fe protein at the desired molar ratio and the second contained 18 mM ATP and 20 mM sodium dithionite. All solutions contained 25 mM HEPES buffer (pH 7.4) and 10 mM $MgCl_2$ and were saturated with N_2.

Preparation of Low-Electron-Flux Rapid-Freeze EPR Samples. Low electron-flux turnover conditions, i.e., an Av1:Av2 molar ratio of 100:1, were used to determine a time course for the decrease in amplitude of the resting EPR signal (signal 1a) of the MoFe protein as described previously (*13*) in the presence of an initial concentration of 18 mM ATP, in addition to 18 mM creatine phosphate and 60 μg/mL creatine phosphokinase, under N_2. After having determined the time needed (about 20 min) to create a sample containing about 50% of the one-electron-reduced MoFe-protein form (E_1) and about 50% of the resting form (E_0), we used the same conditions to generate a similar sample in a rapid-freeze syringe. Immediately after mixing, an initial control sample, which contained E_0 only, was collected by shooting the protein mixture against buffer in the second syringe. After 20 min, the protein mixture was again shot against buffer to demonstrate that only about 50% E_0 remained. The second syringe was then emptied and refilled with Fe-protein solution alone under N_2 at a concentration such that the resulting mixture, after shooting against the E_0/E_1 MoFe-protein solution, would be at a 3:1 Fe protein:MoFe molar ratio. The experimental sample was collected after mixing for 178 ms.

EPR Spectroscopy. X-Band frequency EPR spectra were recorded on a Bruker ESP300 spectrometer operated in perpendicular mode and equipped with an ESR 900 continuous flow helium cryostat (Oxford Instruments). The magnetic field and the microwave frequency were determined with a NMR gaussmeter and a microwave counter. Spectra were recorded at 10 ± 0.2 K with a microwave power of 100 mW and a 100 kHz field modulation of 2 mT. To estimate the uncertainty in the EPR signal intensity introduced by differences in rapid-freeze packing and running-temperature fluctuations, replicate samples, in identical tubes and under constant He flow conditions, gave EPR signals with intensities within ±10% of each other.

Data Analysis and Simulations. The overlapping EPR signals were deconvoluted by computer simulating the

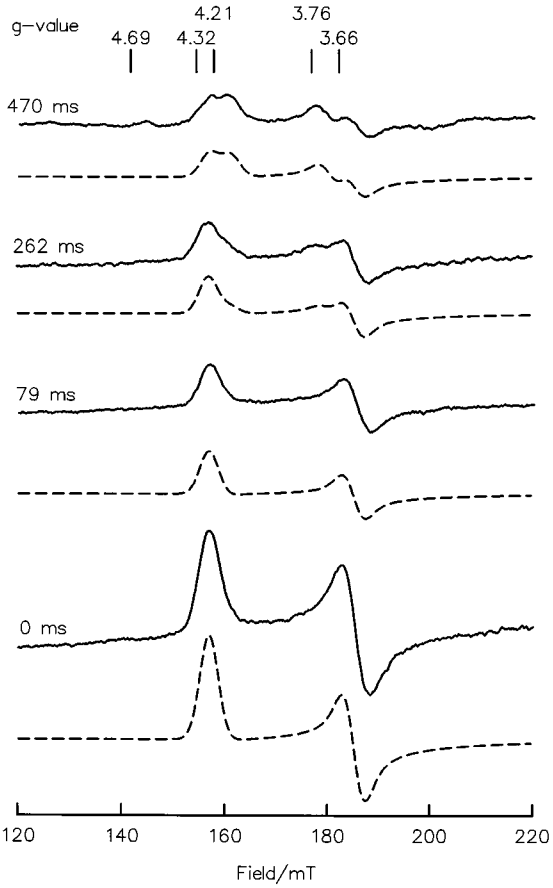

FIGURE 1: Time course for the production of the new EPR signals using a 3:1 Fe protein:MoFe protein molar ratio. Three distinct EPR-active species, which give rise to EPR signals 1a, 1b, and 1c, can be identified during nitrogenase turnover. The characteristic *g* values for signal 1a are 4.32, 3.66, and 2.0; for signal 1b, they are 4.21 and 3.76; and for signal 1c, it is 4.69. Their features close to $g = 4$ are marked. The simulated spectra for signals 1a and 1b are shown as dashed lines directly below each experimental spectrum.

contributions of the g_1 components [signal g_1(a) at $g = 4.32$ and signal g_1(b) at $g = 4.21$] in the EPR spectrum for each of the species present. Representative simulations are shown in Figure 1. Deconvolution and subsequent concentration determinations were more easily performed using the g_1 component rather than the g_2 component (at $g \sim 3.7$). Spectral simulations were performed for both $S = {}^3/_2$ species, 1a and 1b, with each simulation integrating to an intensity of 100% of signal 1a in the buffer-alone sample, i.e., at zero time. The signal heights from each of the simulated 1a and 1b species at both $g = 4.32$ and 4.21 were then measured as H_{1a}, H_{1b*}, H_{1a*}, and H_{1b}, respectively. If a particular spectrum had experimental heights of h_1 at $g = 4.32$ and h_2 at $g = 4.21$, then the contributions, C_a and C_b, for plotting in Figure 2 were obtained by solving the simultaneous equations

$$h_1 = C_a H_{1a} + C_b H_{1b*} \text{ and } h_2 = C_a H_{1a*} + C_b H_{1b}$$

From repeat determinations on the same spectrum, simulation errors are estimated to be ±10%. Time courses for the various species were produced by computer simulations using the Lowe−Thorneley scheme (*12*) and the rate constants therein except for those rate constants that were modified as described below. All EPR data have been corrected to a MoFe-protein concentration of 82 μM and are expressed as

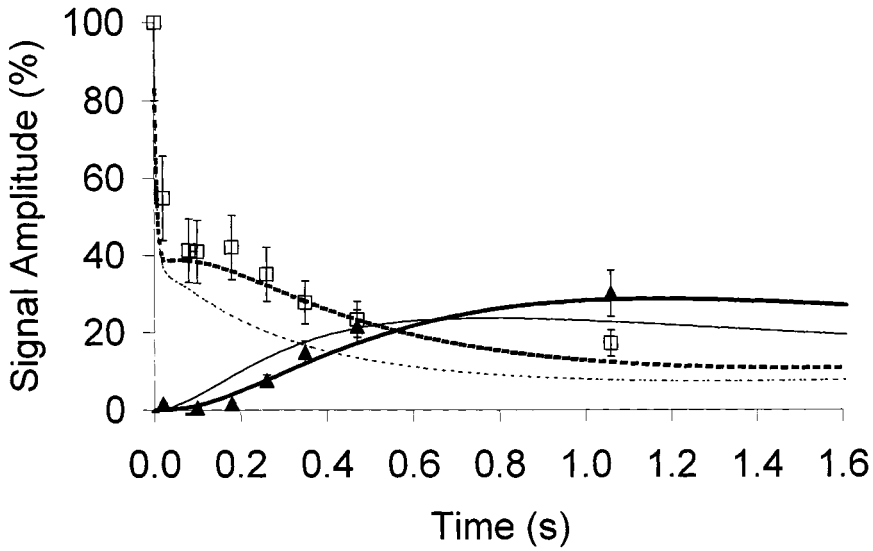

FIGURE 2: Time course for the development of the g_1 component of signal 1a [g_1(a) (□)] and signal 1b [g_1(b) (▲)], during turnover at a 3:1 Fe protein:MoFe protein molar ratio with simulations. The bars represent the estimated ±20% uncertainty in the intensities of the EPR signals. The simulations are based on the Lowe−Thorneley scheme, as described in the text, for the appearance and/or disappearance of the following redox states of the MoFe protein: E_0 (dashed line), E_0 and the E_2−Fe protein(ox) complex before dissociation (bold dashed line), E_2 (solid line), and E_3 (bold solid line).

a percentage of the starting intensity of the resting MoFe-protein EPR signal.

RESULTS AND DISCUSSION

Figure 1 shows typical EPR spectra obtained at a 3:1 Fe protein:MoFe protein molar ratio at various times after initiating turnover. Also shown are the spectra obtained from the simulations described above. At time zero, visualized by shooting the mixture of proteins against buffer not containing ATP, the MoFe protein from *A. vinelandii* at this pH is present as a single species as indicated by the single EPR spectrum (signal 1a) with the following characteristic g values: g_1(a) = 4.32, g_2(a) = 3.66, and g_3(a) = 2.01. Seventy-nine milliseconds after the solution of both proteins had been mixed with MgATP and dithionite to initiate catalysis, the only change evident is a significant (∼60%) bleaching of this starting MoFe-protein signal as an electron is accepted from the Fe protein. After mixing for 262 ms, a new EPR signal (signal 1b) can be observed with the following unique g values: g_1(b) = 4.21 and g_2(b) = 3.76. The magnitude of this new signal continues to increase with time at the expense of the original signal. After mixing for 470 ms, an additional signal (signal 1c) is clearly visible with a g_1(c) of 4.69; however, no accompanying g_2(c) feature could be distinguished. No new features were observed in the $g = 2$ region of any of the spectra at any time after mixing. Similar data were obtained using *K. pneumoniae* nitrogenase proteins under N_2 (data not shown).

Neither changing the substrate present to C_2H_2 nor preparing samples in the absence of N_2, so that the only substrate present was protons, had any significant effect on the formation of these $S = {}^3/_2$ signals (data not shown). Thus, the same forms of the MoFe protein are produced no matter whether the enzyme is accepting two or three electrons (for H^+ and C_2H_2 reduction) or six electrons (for N_2 reduction) during the process of substrate reduction. Apparently, the most-reduced states of the MoFe protein contribute little (or nothing) to the observed EPR spectrum.

Deconvolution of the overlapping EPR signals at g_1, as described in Experimental Procedures, allowed us to plot the time course for the development of each species as shown in Figure 2. Similar, but more scattered, plots were obtained using the g_2 feature. The lines in Figure 2 are computer simulations generated with the Lowe−Thorneley scheme using contributions from various species as described in the legend of Figure 2 and as discussed below.

Unfortunately, we do not have a complete set of rate constants for the *A. vinelandii* nitrogenase; therefore, the assumptions and rate constants that were used were those of Lowe and Thorneley (*12*) for *K. pneumoniae* nitrogenase with the following exceptions. First, the rate of dissociation of Fe protein(oxidized)-MgADP from its complex with the MoFe protein was increased from 6.4 to 11.2 s^{-1} to reflect the higher maximum specific activity of the *A. vinelandii* proteins under these conditions. Second, the rate of the corresponding reverse reaction was increased from 4.4×10^6 to 10×10^6 mol^{-1} s^{-1}. Third, the rate of H_2 release from the MoFe protein in the E_2 redox state was decreased from 250 to 50 s^{-1}. Fourth, the various rate constants associated with N_2 binding were adjusted to improve the fit of the curves to the data.

We then used the simulated curves as indicators of which enzyme species most likely corresponds to the observed EPR signals. Both the quality of the data that can be obtained using rapid-freeze EPR spectroscopy and the lack of a full rate-constant data set limit the precision of our correlations. We estimate that the combination of uncertainties in rapid-freeze packing, EPR running temperature, and the deconvolution/simulation process results in an overall uncertainty of ±20% in each of the data points as recorded in Figure 2. Even so, we feel that useful conclusions can be drawn from the simulations by comparing various hypotheses.

Effect of Electron Flux on EPR Signal Development. The electron flux through the MoFe protein was varied by changing the Fe protein:MoFe protein molar ratio. The resulting changes in the EPR spectrum of the MoFe protein

Table 1: Intensity of Selected EPR Spectral Components as a Function of Electron Flux

Fe protein:MoFe protein molar ratio	time (ms)	g_1(a)[a]	g_1(b)[a]	g_1(c)[a]
5:1	178	1	30	6
	350	2	45	10
1:1	262	92	4	0
	778	89	5	0
	2000	54	5	0
1:3	262	102	5	0
	778	83	8	0
	2000	96	3	0

[a] Intensity of EPR spectral components g_1(a), g_1(b), and g_1(c) of signals 1a, 1b, and 1c, respectively, expressed as a percentage of the intensity of the g_1(a) component in the MoFe-protein sample mixed with buffer alone.

were monitored during catalysis (see Table 1). At low electron flux, generated by a 1:3 Fe protein:MoFe protein molar ratio, an extremely small decrease in the intensity of the resting-state EPR signal 1a [monitored as component g_1(a) of signal 1a] occurred and only a very weak signal 1b [measured as component g_1(b)] was detected at times up to 2 s. When the electron flux was increased, by using a 1:1 Fe protein:MoFe protein molar ratio, about half of the signal 1a intensity was bleached after 2 s, but no compensatory increase occurred in the intensity of signal 1b. Signal 1c, as monitored by component g_1(c), was not detected up to 2 s after mixing under either set of conditions. Under even higher electron-flux conditions, at a 5:1 Fe protein:MoFe protein molar ratio, effectively all signal 1a intensity was bleached 178 ms after mixing. However, neither signal 1b nor signal 1c had yet reached its maximum intensity, although both signals were present. By 350 ms after mixing, both signals 1b and 1c had attained their maximum intensity.

In many experiments, the intensity lost from signal 1a cannot be accounted for by the combined intensities of signals 1b and 1c. This situation is most obvious either after long mixing times or with high electron flux. The data in Table 1 show that, under low-electron-flux conditions, newly appearing signal 1b may account for all of the decreasing intensity of signal 1a. However, even at a 1:1 Fe protein:MoFe protein molar ratio, signal 1a has lost 46% of its intensity after 2 s of mixing with no compensating increase in the intensities of signal 1b and signal 1c. Such observations indicate that EPR-silent species of the MoFe protein are also being produced. One likely candidate is the MoFe protein at the E_1 redox level. It would be formed after H_2 has been evolved from the MoFe protein at the E_3 redox level and may accumulate under either the longer-time or higher-electron-flux conditions. Other candidates, particularly under N_2, could include the most-reduced states of the MoFe protein (at the E_4 redox level and beyond).

Figure 3 shows EPR spectra taken at both a 3:1 and a 5:1 Fe protein:MoFe protein molar ratio after mixing for 350 ms. These results are consistent with those in Table 1. The increased electron flux under the latter conditions clearly resulted in a more rapid and complete conversion of signal 1a into a mixture of signal 1b and signal 1c. This general trend of signal Ib appearing first, followed by signal 1c, under conditions where the MoFe protein is likely to become more reduced, suggests that these signals could arise from more-reduced forms of the MoFe protein. We tested this hypothesis

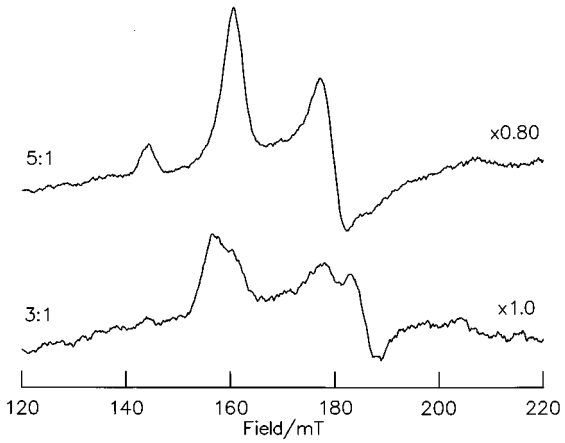

FIGURE 3: Effect of changing electron flux on the time course for development of EPR signals 1b and 1c. The spectra that are shown were recorded 350 ms after mixing, in the presence of excess sodium dithionite, a solution of MgATP with a solution containing the Fe protein and MoFe protein in a molar ratio of either 3:1 (bottom) or 5:1 (top).

by assuming that signals 1a and 1b were given by various combinations of intermediates in the Lowe−Thorneley scheme and then simulating time courses for their appearance (see below).

Formation of EPR Signals from the One-Electron-Reduced MoFe Protein. In a second test of the above hypothesis, we reasoned that, if the MoFe protein was prepared in a more-reduced state before initiating turnover with Fe protein, signals 1b and 1c should appear more rapidly. Attainment of the one-electron-reduced (E_1) level of the MoFe protein can be achieved by using experimental conditions that result in a slow rate of catalytic turnover, namely, with a 1:100 Fe protein:MoFe protein molar ratio. This protocol results in a MoFe-protein solution containing equal proportions of the E_0 and E_1 forms of the MoFe protein. As expected (*13*), the only change observed in the EPR spectrum of the MoFe protein prereduced under these conditions was an ~50% bleaching of the features of signal 1a. This E_0/E_1 protein mixture was then shot against a sufficient excess of Fe protein to give the desired final component:protein ratio. Figure 4 compares EPR spectra obtained by mixing the MoFe protein either in the E_0 resting state or as a 1:1 mixture of the E_0 and E_1 redox states with a 3-fold molar excess of the Fe protein, followed by freeze quenching 178 ms after mixing. As shown in Figure 2, when we started with the MoFe protein in the E_0 resting state, the only change observed in the EPR spectrum after 178 ms was an ~60% decrease in the amplitude of g_1(a). However, when an E_0/E_1 mixture of the MoFe protein reacted with the Fe protein under identical conditions, we observe equal proportions of the 1a and 1b signals after 178 ms. The intensity of each signal was ~33% of the initial intensity of the 1a signal. Clearly, signal 1a decreased faster and signal 1b appeared earlier as a result of this prereduction of the MoFe protein. These observations suggest that the decrease in the intensity of signal 1a is a prerequisite for the formation of signal 1b. This elimination of the early part of the time course, when starting with a more-reduced MoFe protein, is again consistent with signal 1b arising from a MoFe-protein species more reduced than the form which gives rise to signal 1a.

For the reaction starting with the E_0/E_1 mixture, little change in both the relative and absolute proportions of signals

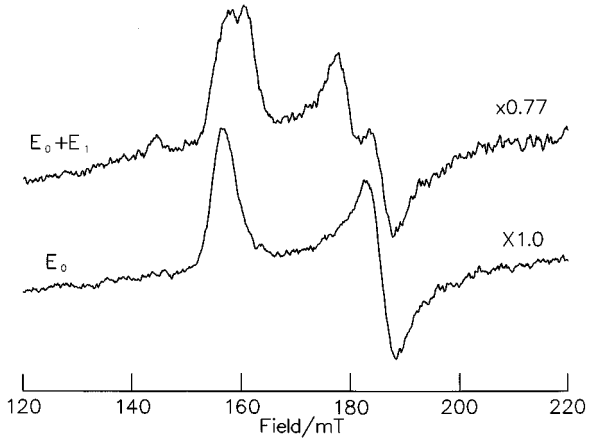

FIGURE 4: Effect of preincubation of the MoFe protein with the Fe protein at a 100:1 molar ratio on the rate of appearance of EPR signals 1b and 1c. Preincubation produces an approximately 1:1 mixture of the E_0 and E_1 redox states of the MoFe protein and, after mixing with a 3-fold excess of Fe protein, results in a more rapid appearance of signals 1b and 1c (top spectrum) than when E_0 is used alone (bottom spectrum). Data were collected after mixing for 178 ms.

1a and 1b was observed 350 ms after mixing, when the intensity of each signal was ~30% of the original intensity of signal 1a. This observation suggests that the system may have reached equilibrium by 178 ms.

Simulated Time Courses. Some time course simulations are shown as lines in Figure 2. As expected, taking free MoFe protein in the E_0 state, plus all the species in equilibrium with it, i.e., E_0 bound to reduced, oxidized, or inactive Fe protein, gives a reasonable fit to both the disappearance and the approach to the steady-state concentration of signal 1a. It is interesting to note that a better simulation is obtained by also including the species with the oxidized Fe protein bound to the MoFe protein at the E_2 redox level. This protein−protein complex forms after the second electron transfer, but before the subsequent dissociation to give the free MoFe protein at the E_2 redox level.

Insight into the nature of the principal species contributing to signal 1b may be gained by analyzing the time courses for the appearance of species in equilibrium with free MoFe protein at either the E_2 or the E_3 redox level as shown in Figure 2. The simulations show that the E_2 species appear too early in the time course. At 178 ms, very little of signal 1b is present in the experimental data, whereas in the simulations, the E_2 species have already risen to about 40% of their equilibrium concentration by this time. We have explored the inclusion and exclusion of many other species in this simulated curve and cannot obtain better fits to the data when the E_2 species are included. This result suggests to us that signal 1b is not a property of the two-electron-reduced MoFe protein.

An examination of the simulated curve for the appearance of the MoFe protein at the E_3 redox level (plus all related species) gives a closer fit to the experimental data for signal 1b. The curve and the data are always close to each other; however, the simulation appears to lead the data up to 300 ms and lag it after this time. These discrepancies could be due either to inadequacies in the scheme, perhaps related to small differences in rate constants associated with the more-reduced states of the MoFe protein, or to the additional reactions that must occur under these conditions.

This correlation between the time courses for the appearance of both signal 1b and the E_3 redox species raises the question of how three electrons can be accommodated within the MoFe protein and still produce an EPR-active species. The simulation based on the Lowe−Thorneley scheme indicates only that three electrons have been accepted; it cannot identify their location. However, all three electrons are unlikely to reside on the FeMo cofactor because this situation should produce an even-electron, EPR-silent species. In any event, signal 1b so closely resembles signal 1a that it almost certainly arises from the FeMo cofactor, suggesting that two of the electrons are associated with the FeMo cofactor whereas the third electron resides either at a location or in a spin state that is not easily EPR-detectable. The fate of this third electron, along with a definitive assignment of the source of the new EPR signal, will be the subject of future investigations.

It is more difficult to estimate which species contributes to signal 1c, because this signal appeared even more slowly than signal 1b and was always weaker under the conditions that we have used. Nevertheless, if our proposal that signal 1b, under these turnover conditions, is elicited from a MoFe protein that is more reduced than that responsible for signal 1a, then signal 1c must arise from a MoFe protein in an even more-reduced redox state than 1b.

We have considered other models to explain the observed changes from signal 1a to signal 1b and then to signal 1c. In the initially most attractive alternative, all three signals were supposed to arise from the MoFe protein at its E_0 redox level (plus all complexed species in equilibrium with E_0 as described above). This model assigned signal 1a to the MoFe protein in its resting (E_0) state, signal 1b to the MoFe protein that had just released H_2 from the E_2 redox level, and signal 1c to the MoFe protein that had released H_2 from state(s) more reduced than E_2. It was also assumed that signals 1b and 1c slowly relax to signal 1a. We used an extensive set of possible rate constants and were able to reproduce roughly the shapes of the curves in Figure 2, but not as well as with the more-reduced protein model discussed above. However, it was impossible to reproduce their amplitudes to within a factor of 2 of the data (not shown). We, therefore, consider this model an inadequate description of the experimental system and reject it.

Implications of the Origins of the Signals. It is generally assumed that the $S = {}^3/_2$ EPR signals elicited from nitrogenase MoFe proteins during the catalytic cycle arise from protein molecules at the E_0 redox level, i.e., in the resting state in equilibrium with dithionite. We have presented evidence above that this assumption may not necessarily be true and that the more-reduced states of the MoFe protein may also contribute to the $S = {}^3/_2$ signals, which may be characterized by different conformations of the FeMo cofactor within the MoFe protein. Signal 1b, the signal with lower rhombicity that we prefer to attribute to MoFe proteins at the E_3 redox level, is equivalent to that reported by Smith et al. (17) for the *K. pneumoniae* MoFe protein at high pH. Under this condition, the altered EPR signal, which likely reflects a corresponding change in conformation, is presumably due to the loss of a proton(s). It is tempting to speculate that, when signal 1b originates from the MoFe protein at the E_3 redox level, it also indicates the loss of a proton(s), which may have been incorporated into the reduced substrate,

such as either bound or free H_2. Moreover, whatever change produces the considerable increase in rhombicity associated with signal 1c, it may also be associated with formation of product.

The observations described in this paper also address an ongoing concern about the relationships among some of the intermediates in the Lowe−Thorneley scheme. In particular, the results provide insight into whether there is any difference between the MoFe protein at the E_0 redox level and the form of the MoFe protein which results immediately after two electrons have relocated to substrate (to form H_2) from what was the E_2 redox level. This relocation of electrons would return the MoFe protein to the E_0 level. The results of our work suggest that the difference in these two forms of the MoFe protein is presumably one of protonation state. In turn, these different protonation states, of either the FeMo cofactor or its immediate environment, could result in different conformations of the FeMo cofactor.

REFERENCES

1. Howard, J. B., and Rees, D. C. (1996) *Chem. Rev. 96*, 2965−2982.
2. Peters, J. W., Stowell, M. H. B., Soltis, S. M., Finnegan, M. G., Johnson, M. K., and Rees, D. C. (1997) *Biochemistry 36*, 1181−1187.
3. Shah, V. K., and Brill, W. J. (1977) *Proc. Natl. Acad. Sci. U.S.A. 78*, 3249−3253.
4. Hawkes, T. R., McLean, P. A., and Smith, B. E. (1984) *Biochem. J. 217*, 317−321.
5. Scott, D. J., May, H. D., Newton, W. E., Brigle, K. E., and Dean, D. R. (1990) *Nature 343*, 188−190.
6. Georgiadis, M. M., Komiga, H., Chakrabarti, P., Woo, D., Kornuc, J. J., and Rees, D. C. (1992) *Science 257*, 1653−1659.
7. Burgess, B. K., and Lowe, D. J. (1996) *Chem. Rev. 96*, 2983−3011.
8. Christie, P. D., Lee, H.-I., Cameron, L. M., Hales, B. J., Orme-Johnson, W. H., and Hoffman, B. M. (1996) *J. Am. Chem. Soc. 118*, 8707−8709.
9. Lee, H.-I., Cameron, L. M., Hales, B. J., and Hoffman, B. M. (1997) *J. Am. Chem. Soc. 119*, 10121−10126.
10. George, S. J., Ashby, G. A., Wharton, C. W., and Thorneley, R. N. F. (1997) *J. Am. Chem. Soc. 119*, 6450−6451.
11. Cameron, L. M., and Hales, B. J. (1998) *Biochemistry 37*, 9449−9456.
12. Lowe, D. J., and Thorneley, R. N. F. (1984) *Biochem. J. 224*, 877−886.
13. Fisher, K., Lowe, D. J., and Thorneley, R. N. F. (1991) *Biochem. J. 279*, 81−85.
14. Thorneley, R. N. F., and Lowe, D. J. (1985) in *Molybdenum Enzymes* (Spiro, T. G., Ed.) pp 222−284, Wiley, New York.
15. Palmer, G., Multani, J. S., Cretney, W. C., Zumft, W. G., and Mortenson, L. E. (1972) *Arch. Biochem. Biophys. 153*, 325−332.
16. Münck, E., Rhodes, H., Orme-Johnson, W. H., Davis, L. C., Brill, W. J., and Shah, V. K. (1975) *Biochim. Biophys. Acta 400*, 32−53.
17. Smith, B. E., Lowe, D. J., and Bray, R. C. (1973) *Biochem. J. 135*, 331−341.
18. Orme-Johnson, W. H., Hamilton, W. D., Ljones, T., Tso, M. Y. W., Burris, R. H., Shah, V. K., and Brill, W. J. (1972) *Proc. Natl. Acad. Sci. U.S.A. 69*, 3142−3145.
19. Smith, B. E., Lowe, D. J., and Bray, R. C. (1972) *Biochem. J. 130*, 641−643.
20. Smith, B. E., and Lang, G. (1974) *Biochem. J. 137*, 169−180.
21. Lowe, D. J., Eady, R. R., and Thorneley, R. N. F. (1978) *Biochem. J. 173*, 277−290.
22. Burris, R. H., and Orme-Johnson, W. H. (1976) in *Proceedings of the First International Symposium on Nitrogen Fixation* (Newton, W. E., and Nyman, C. J., Eds.) Vol. 1, pp 208−233, Washington State University Press, Pullman, WA.
23. Shen, J., Dean, D. R., and Newton, W. E. (1997) *Biochemistry 36*, 4884−4894.
24. Fisher, K., Hare, N. D., and Newton, W. E. (1997) in *Biological Nitrogen Fixation for the 21st Century* (Elmerich, C., Kondorosi, A., and Newton, W. E., Eds.) pp 23−26, Kluwer Academic Publishers, Dordrecht, The Netherlands.
25. Kim, J., and Rees, D. C. (1992) *Science 257*, 1677−1682.
26. Kim, J., and Rees, D. C. (1992) *Nature 360*, 553−560.
27. Chan, M. K., Kim, J., and Rees, D. C. (1993) *Science 260*, 792−794.
28. Bolin, J. T., Campobasso, N., Muchmore, S. W., Morgan, T. V., and Mortenson, L. E. (1993) in *Molybdenum Enzymes, Cofactors and Model Systems* (Stiefel, E. I., Coucouvanis, D., and Newton, W. E., Eds.) pp 186−195, ACS Symposium Series 535, American Chemical Society, Washington, DC.
29. Schindelin, K., Kisker, C., Schlessman, J. L., Howard, J. B., and Rees, D. C. (1997) *Nature 387*, 370−376.
30. Grossman, J. G., Hasnain, S. S., Yousafzai, F. K., Smith, B. E., and Eady, R. R. (1997) *J. Mol. Biol. 266*, 642−648.
31. Grossman, J. G., Hasnain, S. S., Yousafzai, F. K., Smith, B. E., Eady, R. R., Schindelin, H., Kisker, C., Howard, J. G., Tsuruta, H., Muller, J., and Rees, D. C. (1999) *Acta Crystallogr., Sect. D 55*, 727−728.
32. Mayer, S. M., Lawson, D. M., Gormal, C. A., Roe, S. M., and Smith, B. E. (1999) *J. Mol. Biol. 292*, 871−891.
33. Christiansen, J., Tittsworth, R. C., Hales, B. J., and Cramer, S. P. (1995) *J. Am. Chem. Soc. 117*, 10017−10024.
34. Strandberg, G. W., and Wilson, P. W. (1968) *Can. J. Microbiol. 14*, 25−31.
35. Kim, C.-H., Newton, W. E., and Dean, D. R. (1995) *Biochemistry 34*, 2798−2808.
36. Laemmli, U. K. (1970) *Nature 227*, 680−685.
37. Lowry, O. H., Rosebrough, N. J., Farr, A. L., and Randall, R. J. (1951) *J. Biol. Chem. 193*, 265−275.
38. Gutteridge, S., Tanner, S. J., and Bray, R. C. (1978) *Biochem. J. 175*, 869−878.
39. Bray, R. C., Lowe, D. J., Capeillere-Blandin, C., and Fielden, E. M. (1973) *Biochem. Soc. Trans. 1*, 1067−1072.

BI0012686